**Submitted:** 09 August 2018

**Published online in 'accepted manuscript' format:** 05 May 2020

**Manuscript title:** Numerical Modeling of Friction Stir Welding Using Temperature Distribution Obtained from Experiments

**Authors:** Atilla Savaş[1], Mehmet Turgay Pamuk[2], Ömer Seçgin[1], Emrah Arda[3]

**Affiliations:** [1]Faculty of Engineering, Piri Reis University, Istanbul, Turkey. [2]Faculty of Engineering and Natural Sciences, Bahçeşehir University, Istanbul, Turkey. [3]Sakarya University Akyazı Vocational School, Akyazi, Turkey.

**Corresponding author:** Atilla Savaş, Postane Mah. Eflatun Sok. No:8, 34940 Tuzla, Istanbul, Turkey. Tel.: +905425777799

**E-mail:** asavas@pirireis.edu.tr

**Abstract**

In this study, time dependent heat transfer analysis of friction stir welding of AA-6061-T651 plates has been carried out. For this purpose, the COMSOL code is utilized by which the domain is modeled as the rectangular aluminum plate with a moving heat source along the midline. Experimental structure was built in the same manner. The comparison displayed that the advancing condition of the heat source to account for the heat input from the tool shoulder yields realistic results and thus can be a standard for parallel problems. With the help of the steady state model, the heat input for 1500 rpm rotation rate was calculated as 1730 Watts. The results of this work are going to be a reference for future research in this field.

**Notation**

| | |
|---|---|
| $C_p$ | Specific Heat, *J/kg-$^oC$* |
| *CL* | Centreline |
| *E* | Voltage, *Volts* |
| *Exp.* | Experiment |
| *h* | Convective Heat Transfer Coefficient, *W/$m^2$-$^oC$* |
| *I* | Current, *Amperes* |
| *k* | Conductivity, *W/m-$^oC$* |
| *L* | Thickness of the plates, *mm* |
| *m* | Mass*, kg* |
| *P* | Power, *Watt* |
| $q_{shoulder}$ | Heat generated by the shoulder, *Watt* |
| *Q* | Heat, *Watt* |
| $Q_{machine}$ | Heat dissipated to milling machine |
| $Q_{conv.}$ | Heat dissipated by convection |
| $Q_{input}$ | Heat given by the welding tool |
| *T* | Temperature, *$^oC$ or $^oK$* |
| *r* | Radial distance, *m* |
| *t* | Time, *s* |
| *u’’’* | Heat generation*, Watt/$m^3$* |
| *x* | Lateral dimension, *mm* |

| | |
|---|---|
| $y$ | Longitudinal (advancement) dimension, *mm* |

*Greek Symbols:*

| | |
|---|---|
| $\alpha$ | Thermal Diffusion Coefficient, $m^2/s$ |
| $\varepsilon$ | Emissivity, - |
| $\Phi$ | Phase angle, *rad* |
| $\rho$ | Density, $kg/m^3$ |
| $\omega$ | Angular Frequency, *rad/s* |
| $\sigma(T)$ | Temperature Dependent Yield Strength, *Pa* |

*Subscripts:*

| | |
|---|---|
| *inf* | Infinity, sufficiently far away from the domain |
| *net* | Amount left after the losses |
| *conv.* | Convection |
| *load* | Under load condition |
| *idle* | Without load condition |

## 1. Introduction

The FSW process was developed in 1991 by the Welding Institute by Thomas et al. [1] 'A rotating pin, which is attached to a shoulder piece, is moved along the connecting line, which leads to local plastic deformation of the tool and the material. With this method, the welding zone is completely isolated from the atmosphere, which minimizes the formation of voids and large deformations in the welding zone. This new welding technology can be successfully used to connect several structural materials[2-5] and is currently used extensively in the aerospace, automotive and shipbuilding industries.'[6]

Some authors simulated the FSW process with pure thermal models.[7-11] CFD models were also presented.[12-22] In the CFD models, the authors use the Eulerian approach. With Euler's approach, the material flows through the network - or more precisely, the convective contribution due to the material flow is taken into account in the heat equation via the convective term. This method is also known as the "moving coordinate system"

There are also some FSW experiments in previous work.[7-9, 11, 23] These experiments were used either for validation purposes or to improve numerical analysis. For the FSW process, some authors conducted their own experiments[7-9.11] and some used the experiments from previous work [6.24]. This type of validation is used in most numerical applications so that the solutions have a realistic meaning. Other welding methods also used validation. In previous publications, numerical solutions were found for the weld pool [25, 26] and the plasma arc [27, 28] of gas-tungsten arc welding (GTAW) and gas-metal arc welding (GMAW).

In our study, Comsol © 3.5.a was used to solve the heat transfer problem that occurs in

the FSW process of the aluminum alloy AA-6061-T651. In fact, the stationary part of the process is the dwell time of the welding. The first part and the last part of the welding process cannot be accepted as a steady state.

## 2. Theory

Microscopic theories such as the kinetic theory of gases and the theory of free electrons of metals were developed to predict conductivity through media. Continua can be classified according to fluctuations in thermal conductivity. A continuum is said to be homogeneous if its conductivity does not vary from point to point within the continuum, and heterogeneous if there are such variations. In addition, it can be said that the continua in which the conductivity is the same in all directions is isotropic, while those in which the direction change in conductivity is present are called anisotropic. If the Fourier law is introduced into the law of conservation of thermal energy, the differential form of the thermal equation can be obtained solely by temperature. If an isotropic continuum is considered, the following equation is obtained:

$$\rho Cp\, dT/dt = \nabla . (k \nabla T) + u'' \quad (1)$$

where the first term represents the transient part of the energy equation, the second heat conduction and the third heat generation.[29] This general equation can be rearranged with constant $k$ (homogeneous media) at which the heat source moves:

$$dT/dt = V.\nabla T + \alpha \nabla \hat{} 2T + u''/(\rho Cp) \quad (2)$$

where $V$ is the velocity vector and $\alpha$ is the thermal diffusion coefficient. However, for very slow motions such as in the current situation, $V$=0 in Eq. (2) which then becomes same as Eq.

(1). In this case, heat applied is considered to be of time dependent and spatial variation, i.e., $Q_{input} = f(x,y,t)$ which is taken into consideration as a boundary condition.

## 3. Experimental setup

Two pieces of 8 mm-thick Aluminum 6061-T651 plates, both of them having the dimensions of 75x250 mm are welded using Friction Stir Welding method (**Fig. 1**).

The two pieces consist of a 150x250 mm plate when they are welded. A H13 tool steel welding tool is used, which is 30 mm in diameter. The height of the welding tool is 65 mm. The tool is coupled to the spindle of a Milling Machine Model FU 251. A rotational speed of 800 rpm and an advancing rate of 12.5 mm / min was used. We measured the temperatures by an infrared thermometer (GEO Fennel Model Firt 550). The temperature measurement nodes were painted with a black marker to minimize the reflections and keep the emissivity of the surface close to unity ($\varepsilon=1$). We measured the temperatures at every 50 mm in the advancing direction (y) and every 20 mm in the lateral direction (x). Therefore, every 4 minutes, measurements were made which correspond to a feed rate of the welding tool of 12.5 mm / min. The analysis is based on 5 × 7 = 35 temperature measurements at each time step, which is a total of 175 measurements. We calculated the electrical input using the current (I) (11.5 A for loaded case, 8.3 A for idle running) and voltage measurements (V) (380V for both cases) with $P = \sqrt{3}EICos\phi$, using a clamp multimeter, Fluke Model 374. The net input to the experimental range is then calculated as $P_{net}=P_{load}-P_{idle}$ is the actual heat input into the welded parts, where $P_{load}$ and $P_{idle}$ are the electrical power inputs when the load is applied or when the machine is idling.

## 4. Numerical and mathematical model

Heat transfer to and from the experimental domain is calculated using 3-D finite difference transient conduction (**Fig. 2**).

Each unit element representing a differential volume (**Fig. 3**) is assumed to have conduction heat transfer in three dimensions with convection on the upper surface and contact heat loss on the lower surface. Besides a heat input applied by the welding tool is added where the tool is. A heat balance is considered which accounted for the net heat input ($Q_{net}=Q_{input}-Q_{machine}$) where $Q_{input}$ is the amount of heat added due to the friction and $Q_{machine}$ is the heat loss to the machine body where the pieces are clamped onto the machine.

Eq. (2) can then be reformulated into a finite difference equation in three dimensions as follows:

$$Q_{left} + Q_{top} + Q_{right} + Q_{bottom} + Q_{conv.} + Q_{input} + Q_{machine} = mCp\ \Delta T/\Delta t \quad (3)$$

Where $m=\rho V$ is the mass. Since all five terms on the left hand side are related to 2-D conduction and free convection to the environment of temperature $T_{inf}$, they are readily calculated using

$$Q_x = \boldsymbol{kL\Delta y\Delta T/\Delta x} \quad (4)$$

$$Q_y = \boldsymbol{kL\Delta x\Delta T/\Delta y} \quad (5)$$

$$Q_{conv.} = \boldsymbol{h\Delta y\Delta y}\ (T-T_{inf}) \quad (6)$$

Where $L$ is the thickness of the pieces ($L$=8 mm) and $\Delta x$ and $\Delta y$ are the dimensions of the unit element, 20 mm and 50 mm, respectively. Performing the above calculations, net heat input into the experimental domain has been found to be *1500 W* which is comparable to the net

electrical input of

$$P_{net}=P_{load}-P_{idle}=\sqrt{3}\,(380)(11.5)(0.8)-\sqrt{3}\,(380)(8.3)(0.8)=1685W\ (P=\sqrt{3}\,EICos\Phi).$$

The difference of 11% can be explained as the heat loss by axial conduction through the welding tool into the spindle of the milling machine.

*4.1 Finite element modeling*

The model geometry includes three-dimensional pieces in a rectangular coordinate system; a tool and an aluminum plate (250× 150 × 8 mm). The welding tool is an H13 steel 65 mm long, 30 mm in diameter. The attached stirring tool pin is 9 mm in diameter and 7 mm high (**Fig. 4**).

A steady-state model which is independent of time is established. The dwell period of the welding process can easily be simulated by this method. In this modeling approach the welding tool is kept constant and the plates have to be moved in the adverse direction. The energy equation in the present model is solved by Thermal Pseudo Mechanical (TPM) model approach.[11]

*4.2 The heat generated by the shoulder*

The heat generated by the shoulder was given by Eq. (7).[11]

$$q_{shoulder} = \omega r\sigma(T)/\sqrt{3} \quad (7)$$

Here, ω means the rotational speed in rad/s, $r$ shows the radial distance from the center of the tool shoulder in m and $\sigma(T)$ means the temperature dependent yield stress of aluminum alloy in Pa.

Temperature-dependent physical and thermal properties of of AA6061-T651 were reported by Atharifar et al.[30] and are tabulated in Table 1. The constant thermal conductivity, specific heat and density of tool material are given as 42 W/(m K), 500 J/(kg K), and 7800 kg/m3, respectively. Convective heat transfer coefficients are mentioned in section 4.4.

*4.3 The heat dissipated from the tool shoulder to the machine*

This heat dissipation was simulated by choosing a convective heat transfer coefficient according to Schmidt[31] and Larsen et al..[32] This convective heat transfer accounts for the heat dissipated to the milling machine which is approximately 10 % of the heat generated. The chosen coefficient at the upper part of the tool is 10.000 $W/m^2 K$. The other boundaries of the tool were selected as thermally insulated. The upper part of the tool which can be seen from Fig. 4 where the "CW Rotation" tag was placed is so arranged that the convective heat transfer coefficient was taken as 10.000 $W/m^2 K$. This is done on purpose for generating a 10 % heat dissipation from tool to the milling machine. By doing so the temperature distribution is maintained close to the experimental values.

*4.4 The convective heat transfer coefficient from top of the plates to the air*

Upper convective heat transfer coefficient was taken as 6 $W/m^2 K$ and lower convective heat transfer coefficient was taken as 200 $W/m^2 K$. Backing plate is not included in our work like many researchers do. The heat transfer to the backing plate was simulated by a high convective heat transfer coefficient. The workpiece-backing plate contact is responsible for the majority of the heat loss from the workpiece during FSW and is discussed by Larsen[32] in his work. Typical

values of heat transfer coefficients used in the literature are around 200-400. The convective heat transfer coefficient for upper part of the plate was mention in the same work as around 10 6 W/$m^2$ K. For good calibration purposes the upper coefficient was taken as 6 W/$m^2$ K and the lower coefficient was taken as 200 W/$m^2$ K. Therefore we could get temperature distribution close to the experimental ones.

## 5. Results

**Fig.s 5** through **9** obtained using Matlab© show the temperature distribution as the stirring tool advances. **Fig 10** shows the comparison of experimental field measurements with those of Comsol© results. Nandan[20] explained the method for which the transient temperature distribution from the experiment can be transformed to steady state temperature distribution by a simple operation. Horizontal axis in the transient results which represent the time in seconds can easily be transformed to displacements by multiplying it by the welding velocity. By doing so both temperature distributions can easily be compared As can be seen from the field temperature measurements, heat is diffused primarily in the advancement direction and then in the retreating side. Same tendency can be observed in the numerical results. **Fig. 11** shows the rotational speed dependence of heat generated during the process. The heat generated at high rotational speeds causes the maximum temperature at the welding zone to get higher. This behavior was also observed in the work of Serindağ et al..[33] The temperature distributions for 600 rpm and 1.33 mm/s welding condition is shown in **Fig. 12**. As mentioned earlier the peak temperature increases as the rotation rate is increased. But as the peak temperature approaches the melting temperature, the rate of increase of the temperature slows down, because the

friction forces diminish as the metal softens.

## 6. Conclusion

The modeling of the friction stir welding process was carried out by a number of researchers. The literature contains thermal and CFD models, thermal CSM (Computational Solid Mechanics) and pure thermal models. In our experimental and numerical work, we used a simple temperature measurement scheme and used the measured temperature data to temporarily analyze the welding process using the finite difference method. We also created a stationary finite element model to predict the heat input with increasing tool speed. The minimum heat input for the tool speed of 800 rpm was 1500 watts, while the maximum heat input from the tool speed of 1500 rpm was approximately 1730 watts. This simple experimental setup can help a welding engineer calibrate his finite element model and predict the thermal behavior of the welded plates. The introduction of this method can eliminate expensive and time-consuming data acquisition systems, but one must take into account the compromise between the simplicity and the quality of the measurements.

**References**

1. Thomas MV, Nicholas J, Needham JC, Murch MG, Templesmith P and Dawes CJ: 1991 Friction stir butt welding GB Patent Application no. 9125978-8, 1991; US Patent no. 5460317.
2. Çam G, and İpekoğlu, G (2017) Recent developments in joining of aluminium alloys, Int. J. Adv. Manuf. Technol., 91(5-8) 1851-1866
3. Çam G, and İpekoğlu, G, Küçükömeroğlu, T, and Aktarer, SM (2017) Applicability of friction stir welding to steels, Journal of Achievements in Materials and Manufacturing Engineering (JAMME), 80(2): 65-85
4. Çam, G and Mıstıkoğlu, S (2014) Recent developments in friction stir welding of Al-alloys, Journal of Materials Engineering and Performance (JMEPEG), 23 (6): 1936-1953
5. Çam, G (2011) Friction stir welded structural materials: Beyond Al-alloys, Int. Mater. Rev., 56 (1): 1-48
6. Roy B.S, Saha S.C and Barma J.D ,2012 "3-D Modeling & Numerical Simulation of Friction Stir Welding Process" *Advanced Materials. Research*, 488-489, 1189–1193. https://doi.org/ 10.4028/www.scientific.net/AMR.488-489.1189
7. Chao Y.C., Qi X. and Tang W. ,2003, "Heat Transfer in Friction Stir Welding—Experimental and numerical studies" *International Journal of Manufacturing Science and Engineering*, 125, (1), 138–145.doi:10.1115/1.1537741
8. Song M and Kovacevic R 2003a "Numerical and experimental study of the heat transfer process in friction stir welding" *Proceedings of Institute of Mechanical Engineering B*,

217B, 73–85. doi: https://doi.org/10.1243/095440503762502297

9. Song M and Kovacevic R 2003b "Thermal modeling of friction stir welding in a moving coordinate" *International Journal of Machine Tools Manufacturing*, 43, 605–615. doi: https://doi.org/10.1016/S0890-6955(03)00022-1
10. Schmidt H.B and Hattel J.H, 2004 "Heat Source Models in Simulation of Heat Flow in Friction Stir Welding", *International Journal of Offshore Engineering.,* 14, (4), 296–304.
11. Schmidt HB and Hattel JH 2008a "Thermal and Material Flow modelling of Friction Stir Welding with COMSOL", Excerpt from the Proceedings of the COMSOL Conference, Hannover (CD-ROM).
12. Colegrove P.A. Painter M., Graham D. and Miller T., 2000 "3D Flow and Thermal Modeling of theFSW Process", 2nd Int. Symp. of FSW Proc. 2nd Int. Symp. on 'Friction stir welding', Gothenburg, Sweden, June (CD-ROM), TWI Ltd.
13. Seidel T.U and Reynolds A.P ,2003 "Two-dimensional friction stir welding process model based on fluid mechanics" *Science and Technology of Welding and Joining* 8, (3), 175–183.
14. Colegrove P.A. and Shercliff H.R., 2004 "Two-dimensional CFD modelling of flow round profiled FSW tooling", *Science and Technology of Welding and Joining,* 9, (6), 483–492. doi: https://doi.org/10.1179/136217104225021832
15. Colegrove P.A and Shercliff H.R, 2006 "CFD modelling of friction stir welding of thick plate 7449 aluminum alloy", *Science and Technology of Welding and Joining* 11, (4), 429–441. doi: https://doi.org/10.1179/174329306X107700

16. Long T and Reynolds A.P ,2006 “Parametric studies of friction stir welding by commercial fluid dynamics simulation”, *Science and Technology of Welding and Joining* 11, (2), 200–208. doi:https://doi.org/10.1179/174329306X85985

17. Nandan R, Roy GG and Debroy T 2006 “Numerical simulation of three-dimensional heat transfer and plastic flow during friction stir welding*”, Metallic Materials Transactions. A: Physics of Metallic Materials Science* 37, (4),1247.1259.doi:https://doi.org/10.1007/s11661-006-1076-9

18. Nandan R, Roy GG, Lienert TJ and Debroy T, 2007 “Three-dimensional heat and material flow duringfriction stir welding of mild steel”, *Acta Materiala.,* 55, 883–895. doi: https://doi.org/10.1016/j.actamat.2006.09.009

19. Dörfler D.M 2008 Advanced modeling of friction stir welding – improved material model for aluminum alloys and modeling of different materials with different properties by using the level set method’, Excerpt from the Proceedings of the COMSOL Conference, Hannover (CD-ROM).

20. Nandan R ,2008 “Computational modeling of heat transfer and visco-plastic flow in friction stir Welding” PhD thesis, The Pennsylvania State University, PA, USA, 17-25.

21. Reynolds A.P, 2008 “Flow visualization and simulation in FSW”, *Scripta Materiala*, 58, 338–342. doi: https://doi.org/10.1016/j.scriptamat.2007.10.048

22. Hattel J.H, Schmidt H.B and Tutum C., 2010 “Thermomechanical Modelling of Friction Stir Welding” Trends in Welding Research, Proc. 8th Int. Conf. 1–10

23. Cambridge University Website http://www-materials.eng.cam.ac.uk/FSW_Benchmark/,

accessed on 1.3.2013.

24. Atallah MM (2007) "Microstructure-property development in friction stir welds of aluminum-based Alloys", PhD thesis, University of Birmingham, UK,
25. Hu J, Guo H and Tsai H.L,2008 "Weld pool dynamics and the formation of ripples in 3D gas metal arc Welding", *International Journal of Heat and Mass Transfer,* 51, 2537–2552. doi: https://doi.org/10.1016/j.ijheatmasstransfer.2007.07.042
26. Traidia A and Roger F, 2011 "Numerical and experimental study of arc and weld pool behavior for pulsed current GTA welding", *International Journal of Heat and Mass Transfer,* 54 2163–2179. doi: https://doi.org/10.1016/j.ijheatmasstransfer.2010.12.005
27. Hu J; Tsai H.L and Wang P.C, 2006 "Numerical modeling of GMAW arc" *Advanced Computer Information, System Science and Engineering,* 69–74.
28. Savas A and Ceyhun V , 2012 "Finite element analysis of GTAW arc under different shielding", *Computational. Materials Science.*, 51, (1), 53-71. doi: https://doi.org/10.1016/j. commatsci.2011.07.032
29. Arpaci V.S. 1966 *Conduction Heat Transfer*, New York Addison Wesley, 32-36.
30. Atharifar H, Lin D, and Kovacevic R , 2009 "Numerical and experimental investigations on the loads carried by the tool during friction stir welding", *Journal of Materials Engineering Performance* 18, (4), 339–350. doi: https://doi.org/10.1007/s11665-008-9298-1
31. Schmidt H.B 2010 "Modelling thermal properties in friction stir welding," D. Lohwasser and Z. Chen (Eds.), Friction stir welding from basics to applications; Woodhead

Publishing, UK, pp. 277–313.

32. Larsen A, Stolpe M and Hattel J.H , 2012 “Estimating the workpiece-backing plate heat transfer coefficient in friction stir welding”, *Engineering Computation and Journal of CAE Software*, 29, (1), 65–82. doi: https://doi.org/10.1108/02644401211190573

33. Serindağ H.T, Kiral B.G and Kadayifçi Z.A (2014) Finite Element Analysis of friction stir welded aluminum alloy AA6061-T6 joints, Material Testing 56 (11-12), pp.937-944, DOI:org/10.3139/120.110653

**Table 1.** Temperature-dependent material properties of AA 6061-T6 used in CFD model[30]

| Temperature,K | Density,kg/m$^3$ | Thermal conductivity, W/m C | Heat capacity, J/Kg C | Yield strength, MPa |
|---|---|---|---|---|
| 273 | 2700 | 162 | 917 | 277.7 |
| 366.3 | 2685 | 177 | 978 | 264.6 |
| 477.4 | 2657 | 192 | 1028 | 218.6 |
| 588.6 | 2630 | 207 | 1078 | 66.2 |
| 700.7 | 2602 | 223 | 1133 | 17.9 |
| 844.1 | 2574 | 253 | 1230 | 0 |

**Figure 1.** Experimental setup

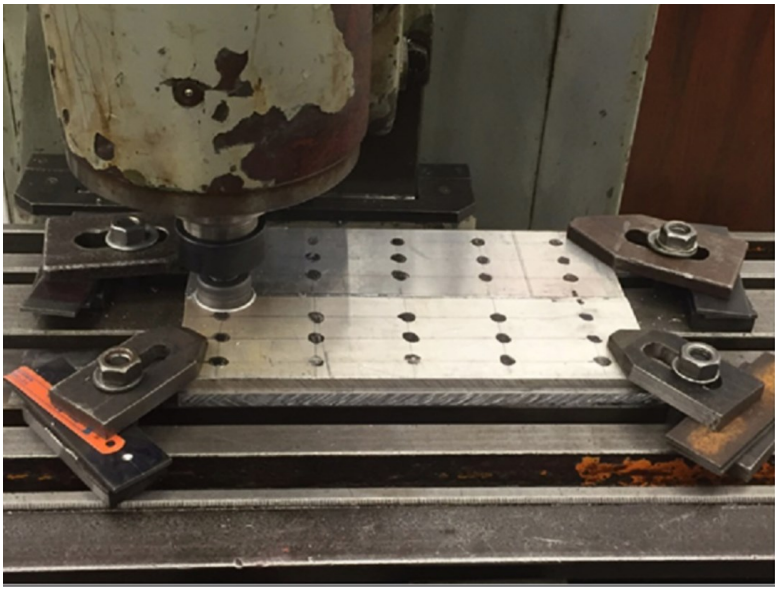

**Figure 2.** Experimental domain

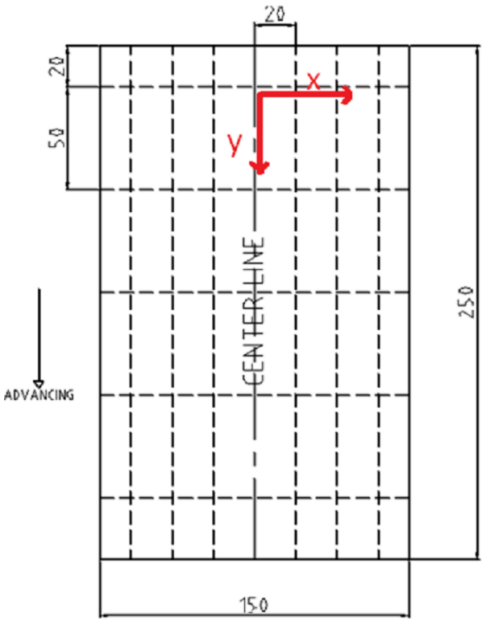

**Figure 3.** Unit element of 20x50 mm.

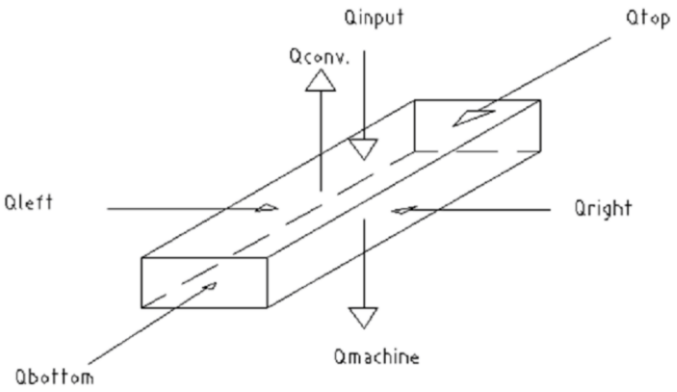

**Figure 4.** Computational domain

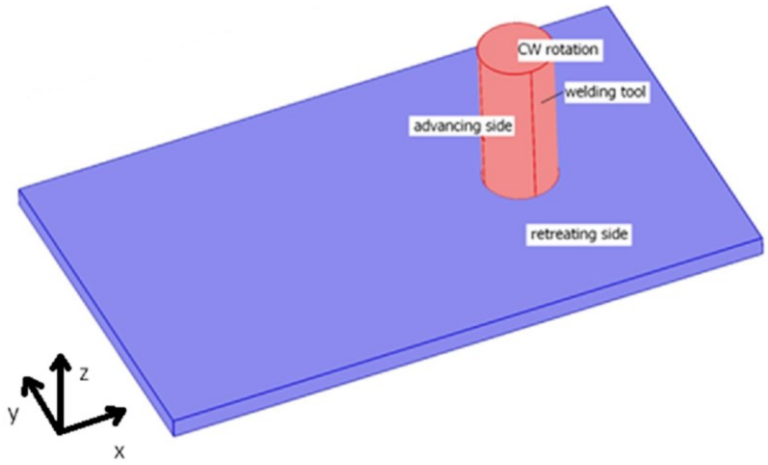

**Figure 5.** Temperature distribution t=0 min.

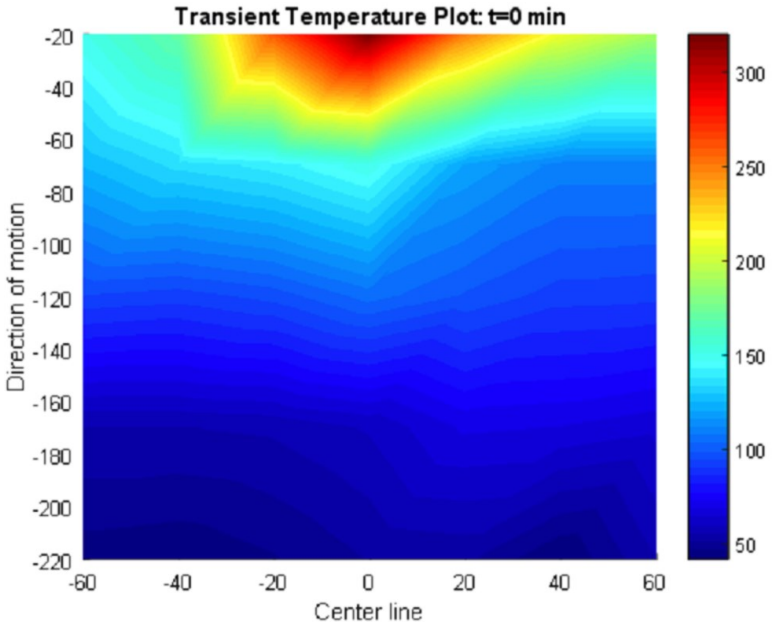

**Figure 6.** Temperature distribution t=4 min.

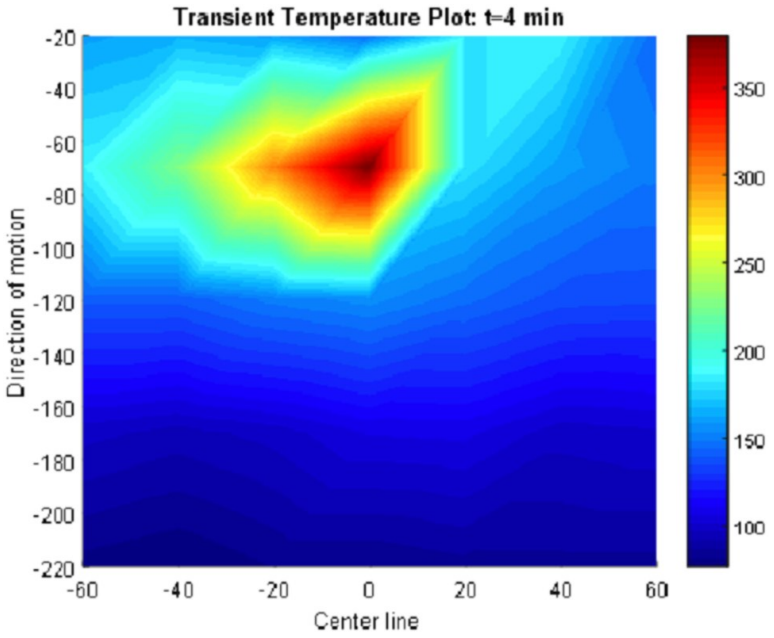

Accepted manuscript
doi: 10.1680/jemmr.18.00080

**Figure 7.** Temperature distribution t=8 min.

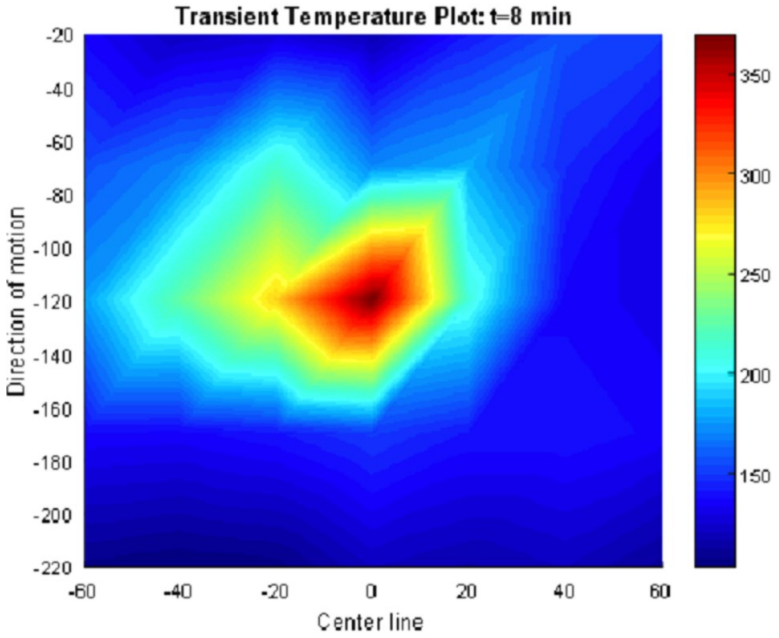

Accepted manuscript
doi: 10.1680/jemmr.18.00080

**Figure 8.** Temperature distribution t=12 min.

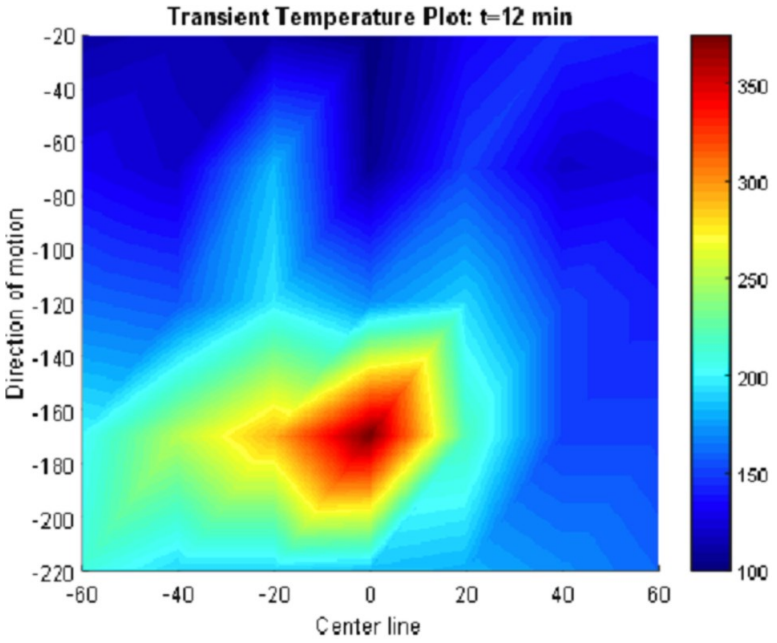

Accepted manuscript
doi: 10.1680/jemmr.18.00080

**Figure 9.** Temperature distribution t=16 min

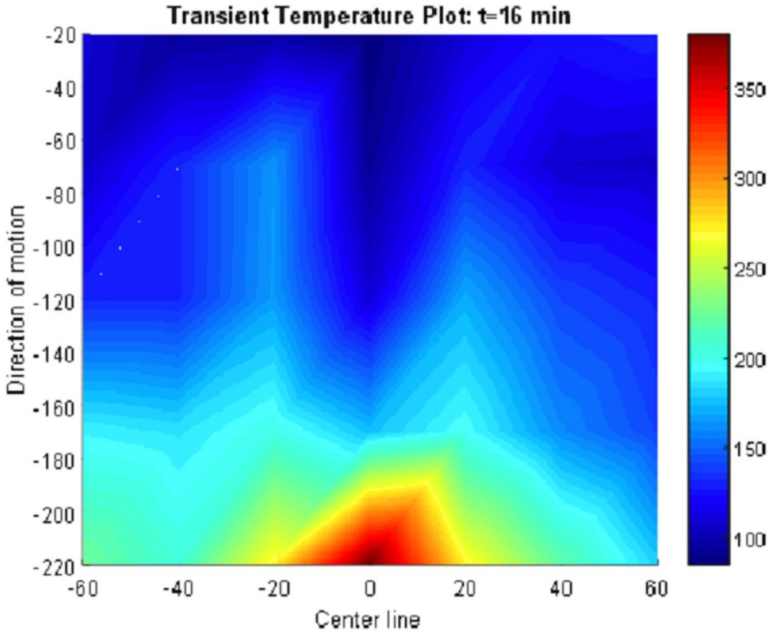

Accepted manuscript
doi: 10.1680/jemmr.18.00080

**Figure 10.** Comparison of results. (40 mm away from the centerline on the retreating side)

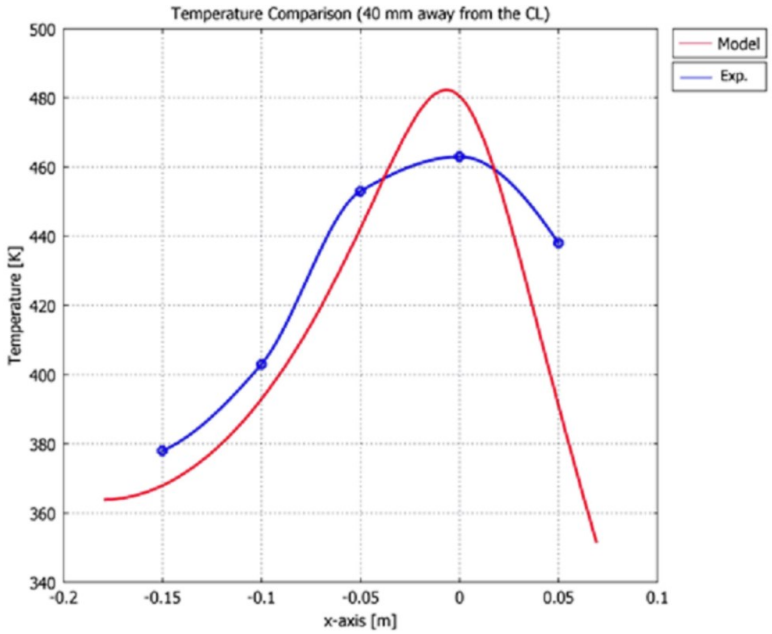

**Figure 11.** The heat applied by the shoulder with changing tool rotation rate

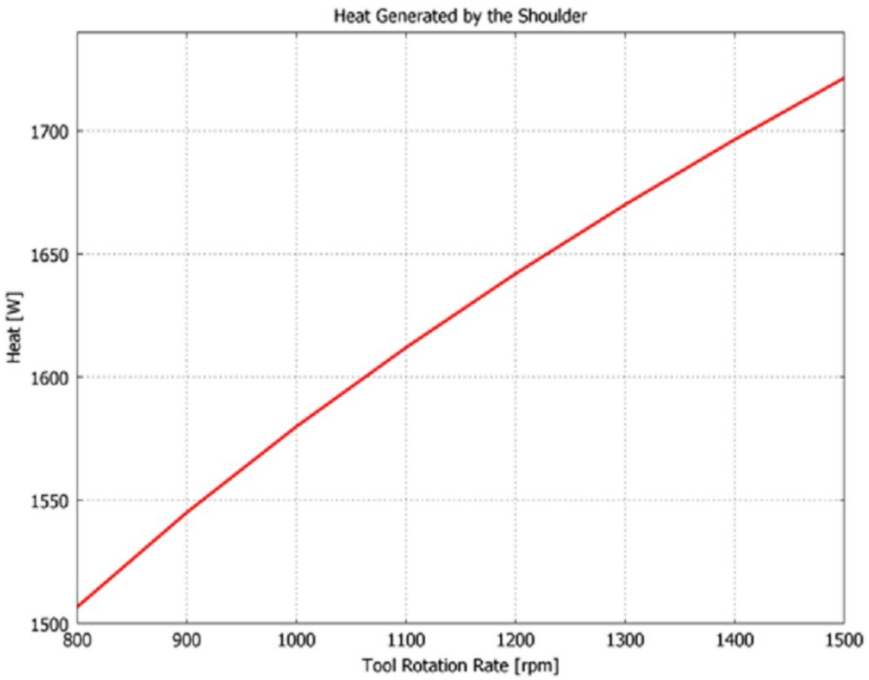

Accepted manuscript
doi: 10.1680/jemmr.18.00080

**Figure 12.** The temperature distribution at the welding conditions 600 rpm and 1.33 mm/s